Available online at www.sciencedirect.com
SCIENCE DIRECT
Cement and Concrete Research 36 (2006) 697 – 706
Cement and Concrete Research

Effect of ettringite on thaumasite formation

S. Köhler *, D. Heinz, L. Urbonas

Centre for Building Materials, Technical University Munic, Baumbachstr. 7, 81245 Munic, Germany

Received 29 June 2005; accepted 7 November 2005

Abstract

Deterioration of cementitious building materials is often caused by sulphate attack where ettringite and gypsum play the most destructive role at moderate ambient temperatures. In contrast, thaumasite $[Ca_3Si(OH)_6{\cdot}12H_2O](SO_4)(CO_3)$ is mostly observed at comparatively low temperatures of less then 15 °C. This mineral forms from calcium, sulphate, carbonate and silicon. The latter originates from the decomposition of C–S–H which results in deterioration of the hardened cement paste structure. To investigate the effect of ettringite on thaumasite formation, pastes were mixed using synthetic clinker phases, fly ash and nanosilica. Aqueous suspensions were prepared with the ground-hydrated pastes mixed with calcite and either gypsum or sodium sulphate. Following different storage periods, the solid phase was separated by filtration, dried and analysed by XRD using the Rietveld method as well as ESEM and TEM. The liquid phase was analysed by ICP-OES. The results indicate that thaumasite formation occurs through the heterogeneous nucleation of thaumasite on the surface of ettringite, due to the structural similarities of these minerals. This reaction is followed by further epitaxial growth of thaumasite from its components present in solution.
© 2005 Elsevier Ltd. All rights reserved.

Keywords: Thaumasite; Ettringite; Sulphate attack

1. Introduction

It has been known for many years that sulphate attack can result in the deterioration of cementitious materials in construction components. Apart from the well-known reaction products ettringite and gypsum, thaumasite $[Ca_3Si(OH)_6{\cdot}12H_2O](SO_4)(CO_3)$ is mostly observed to form in the presence of carbonate at temperatures below 15 °C. In few cases, thaumasite was found at higher temperatures, for instance, in Southern California [1]. As well as carbonate and sulphate, thaumasite contains silicon which is mostly derived from the decomposition of C–S–H [2]. Due to this process, the cement paste matrix transforms into a soft mushy incohesive mass [2,3] and this can be a serious problem. For example, in 1998, extensive damage was discovered in the 30-year-old foundations of UK motorway bridges [2]. Since then, increasing attention has been focused on the formation of thaumasite and deterioration in consequence of this type of sulphate attack.

Thaumasite forms a solid solution with ettringite which is usually present in cementitious materials [4–7]. Investigations to explain the formation route of thaumasite with and without participation of ettringite were undertaken by several authors [3,8–11]. According to Bensted [9–11], thaumasite forms either from the decomposition of ettringite and C–S–H via precipitation of the intermediate phase woodfordite (woodfordite route) or directly from the solution. Crammond [3] offers three different theories. (1) Thaumasite forms through a topochemical interchange of $[Si^{4+}]$ for $[Al^{3+}]$ and $[CO_3^{2-}+SO_4^{2-}]$ for $[SO_4^{2-}+H_2O]$. From the released aluminium in combination with available SO_4^{2-} and Ca^{2+} secondary ettringite is formed. (2) Formation of thaumasite occurs directly from the pore solution. In this case, primary sulphate reacts with aluminate forming ettringite. Thaumasite will then precipitate if carbonate as well as sulphate is available and the total amount of aluminate has been exhausted by the ettringite formation. In this environment, the solubility of thaumasite is lower than the solubility of C–S–H, and therefore, C–S–H dissolves in favour of the formation of thaumasite. (3) Thaumasite uses ettringite as a template for its initial nucleation. Several workers observed the occurrence of thaumasite for cements of different composition [12–17]. In

* Corresponding author.
E-mail address: sibylle_koehler@yahoo.com (S. Köhler).

0008-8846/$ - see front matter © 2005 Elsevier Ltd. All rights reserved.
doi:10.1016/j.cemconres.2005.11.006

Table 1
Composition of mixtures (wt.%)

	C_3S	Alite	C_3A	C_4AF	Gypsum	Fly ash	SiO_2
A1	100						
A2		100					
A3		77	8		15		
A4		85	8		7		
A5		85		8	7		
A6		80				20	
B1		83					17
B2		67	7		13		13
B3		73	7		6		14
B4		73		7	6		14
C1		65					35
C2		55	5		11		29
C3		58	6		5		31
C4		58		6	5		31

Pastes were prepared at two different Na_2O_{eq} (0 and 0.5 wt.%).
A without addition of SiO_2 (Aerosil®), C/S=3.0, *w/s*=0.5.
B with addition of SiO_2 (Aerosil®), C/S=1.7, *w/s*=1.
C with addition of SiO_2 (Aerosil®), C/S=1.0, *w/s*=3.

view of the varied compositions of cements as well as the large and often undocumented differences in environmental conditions, it is not surprising that evidence is provided for all theories. In this paper, the results of investigations with mixtures of synthetic clinker minerals with calcite and sulphate are presented. The aim is to find out more about the formation process of thaumasite by using the basic phases in a methodical way.

2. Materials and methods

2.1. Preparation of basic materials

The synthesis of the clinker phases alite, C_3S, C_4AF and C_3A was carried out by sintering stoichiometric mixtures of basic materials (pro analysi purity) in the laboratory. The alite contained 1 wt.% Fe_2O_3, Al_2O_3 and MgO, respectively. Additionally, SiO_2 (7 nm Aerosil®, Degussa) and fly ash were used for the experiments. Ettringite was synthesised according to Atkins et al. [18] from a slurry of CaO and $Al_2(SO_4)_3 \cdot 18H_2O$; the Ca/SO_4 and *w/s* ratios were 2 and 10, respectively. The water was boiled in a N_2 atmosphere to remove CO_2 and thus reduce the carbonatisation of $Ca(OH)_2$ later on. The slurry was rotated at about 30 revolutions/min for 7 days at room temperature. Afterwards, the slurry was dried and analysed by X-ray diffraction (XRD) using the Rietveld method. The dry material was found to contain 99 wt.% ettringite and 1 wt.% gypsum.

2.2. Preparation of suspensions based on hydrated pastes of clinker phases

Two series of pastes were prepared by mixing the basic materials at the proportions in Table 1 either with water or with a KOH solution to give an alkali equivalent of 0.5 wt.% with respect to the total solid phases. Each series contained groups of pastes with *w/s* ratios of 0.5, 1.0 and 3.0. Different ratios of C/S=1 and 1.7 were set by means of nanosilica addition. The pastes were stored in closed plastic containers at 22 °C.

The hydration of all pastes was stopped with isopropanol after 28 days. Afterwards, the hardened pastes were ground with isopropanol and the powder dried for approximately 10 h at 50 °C to ensure complete evaporation of the isopropanol.

Suspensions with a *w/s* ratio of 10 were prepared by mixing the ground pastes with water, calcite and either gypsum or Na_2SO_4. Sodium sulphate was used to investigate the effect of higher concentrations of sulphate in solution. The amounts of calcite and gypsum used were calculated from the available SiO_2 according to the stoichiometry of thaumasite. Na_2SO_4 was added in the mixing water which contained 4.4 g/l (3 g/l SO_4^{2-}). The suspensions were stored at 5 and 10 °C. After 56 days, Na_2SO_4 was added to the suspensions made with Na_2SO_4 solution, resetting the concentration to 3 g/l SO_4^{2-}. The stages of sample preparation and the storage conditions are summarised in Fig. 1.

After 28, 56, 120 and 365 days the suspensions were shaken and in each case approximately 15 ml samples taken for analysis. The fluid was separated from the solid by filtration and the hydration of the solid material was stopped with isopropanol. Afterwards, the solid material was dried at 50 °C for approximately 1 h.

2.3. Preparation of suspensions based on hydrated pastes of C_3S

In order to investigate the formation route of thaumasite from ettringite via woodfordite, suspensions were prepared using dried and ground hydrated C_3S powder, synthetic ettringite and calcite. The hydrated C_3S powder was prepared using water (without KOH) in same manner as the samples in

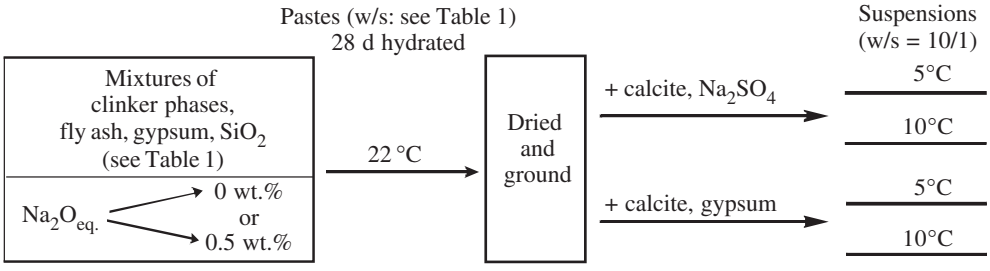

Fig.1. Procedure for sample preparation and shortage.

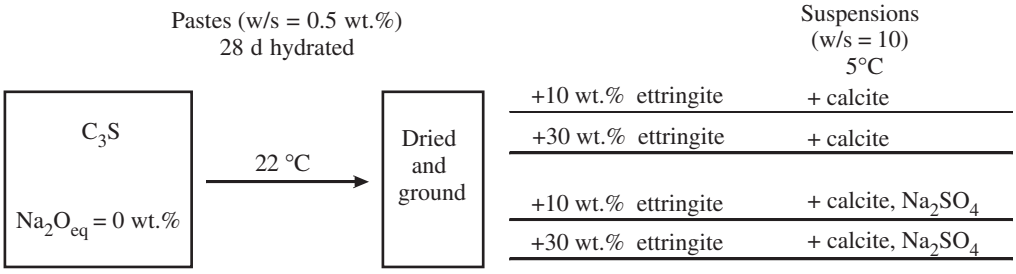

Fig. 2. Preparation and storage of the hydrated C_3S pastes mixed with ettringite, calcite and Na_2SO_4 solution.

Section 2.2. Synthetic ettringite was added to hydrated C_3S at proportions of either 10 wt.% or 30 wt.% with respect to total solids. Calcite was then added to each mixture according to the stoichiometry of SiO_2 in thaumasite. Suspensions were prepared with the four mixtures using either bidistilled water or a solution of Na_2SO_4 (3 g/l SO_4^{2-}). Fig. 2 shows the procedure for sample preparation and the storage conditions. After storage periods of 7, 14, 28 and 56 days, solid samples for analysis were prepared as described in the previous section.

2.4. Analytical methods

The solid materials were analysed by X-ray powder diffraction (XRD) with Rietveld analysis as well as environmental scanning electron microscopy and transmission electron microscopy (ESEM and TEM). For XRD, the samples were carefully ground by hand in an agate mortar. Isopropanol was used as a grinding medium to avoid destruction of the crystal structures of aqueous minerals. The material was passed through a sieve with mesh size 32 μm. The phase analyses by XRD were carried out using a theta–theta goniometer (GE Inspection Technologies) with CuK_α radiation (40 kV, 40 mA). The quantitative analysis of the phases in the samples was carried out with the Rietveld software Autoquan produced by the same company. Investigations with ESEM as well as TEM were carried out with a FEI XL30 FEG at 250 kV and a JEOL JEM 100 CX (100 kV) microscope, respectively. The solid material was spread on films of carbon.

3. Results and discussion

In general, an increase in the volume of the precipitate was observed in suspensions in which thaumasite was detected. Samples stored at 5 °C possessed more distinct reflections of thaumasite than samples kept at 10 °C which indicates a trend towards increased thaumasite formation at lower temperatures. The alkali equivalent of the paste did not affect the pH values significantly. In general, the values echo the known effect of temperature and solubility of the various solid phases in the individual suspensions. The pH values of mixtures with nanosilica are up to 0.2 units lower than pH values of mixtures without nanosilica. According to [19] the equilibrium pH for thaumasite solubility in water is 8.19. Nevertheless, a large decrease in pH of the suspension solutions is not apparent (see Tables 2 and 3).

3.1. Results for suspensions A without additional SiO_2

The total absence of thaumasite after 365 days in samples without aluminate as well as ettringite is noteworthy. Traces

Table 2
Occurrence of mineral phases and pH values in samples taken from suspensions A, temperature of storage: 5 and 10 °C, after 365 days

Source of sulphate in the suspension: gypsum (5 °C/10 °C)						
	A1	A2	A3	A4	A5	A6
$Na_2O_{eq.}$ = 0 wt.%						
Alite/C_3S	X/X	–/–	–/–	–/–	–/–	–/–
Gypsum	X/X	X/X	X/X	X/X	X/X	X/X
Calcite	X/X	X/X	X/X	X/X	X/X	X/X
Aragonite	X/X	–/–	–/–	–/–	–/–	–/–
Ettringite	–/–	X/X	X/X	X/X	X/X	X/X
Portlandite	X/X	X/X	X/X	X/X	X/X	X/X
Thaumasite	–/–	X/X	X/X	X/X	X/X	X/–
pH value	12.5/12.8	12.8/12.9	13.1/12.6	13.1/12.5	12.9/12.9	12.7/12.4
$Na_2O_{eq.}$ = 0.5 wt.%						
Alite/C_3S	X/X	–/–	–/–	–/–	–/–	–/–
Gypsum	X/X	X/X	X/X	X/X	X/X	X/X
Calcite	X/X	X/X	X/X	X/X	X/X	X/X
Aragonite	X/X	–/–	–/–	–/–	–/–	–/–
Ettringite	–/–	X/X	X/X	X/X	X/X	X/X
Portlandite	X/X	X/X	X/X	X/X	X/X	X/X
Thaumasite	–/–	X/X	X/X	X/X	X/X	X/X
pH value	13.1/12.9	13.0/12.9	13.0/12.8	13.0/12.8	13.1/12.8	12.7/12.8
Source of sulphate in the suspension: Na_2SO_4 (5 °C/10 °C)						
$Na_2O_{eq.}$ = 0 wt.%						
Alite/C_3S	X/X	–/–	–/–	–/–	–/–	–/–
Gypsum	–/–	–/–	–/–	–/–	–/–	–/–
Calcite	X/X	X/X	X/X	X/X	X/X	X/X
Aragonite	X/X	–/–	–/–	–/–	–/–	X/–
Ettringite	–	X/X	X/X	X/X	X/X	X/X
Portlandite	X/X	X/X	X/X	X/X	X/X	X/X
Thaumasite	–/–	X/–	X/X	X/–	X/X	–/–
pH value	13.1/13.1	13.1/13.1	13.2/13.0	13.3/13.1	13.3/13.1	13.3/13.1
$Na_2O_{eq.}$ = 0.5 wt.%						
Alite/C_3S	X/X	–/–	–/–	–/–	–/–	–/–
Gypsum	–/–	–/–	–/–	–/–	–/–	–/–
Calcite	X/X	X/X	X/X	X/X	X/X	X/X
Aragonite	X/X	–/–	–/–	–/–	–/–	X/X
Ettringite	–/–	X/X	X/X	X/X	X/X	X/X
Portlandite	X/X	X/X	X/X	X/X	X/X	X/X
Thaumasite	–/–	X/–	X/X	X/–	X/X	–/–
pH value	13.0/13.0	13.4/13.1	13.3/13.3	13.2/13.0	13.4/13.1	13.4/13.0

Presence of phase is denoted by X.

Table 3
Mineral phases and pH values of samples from suspensions with pastes B and C, temperature of storage: 5 and 10 °C, after 365 days

Source of sulphate in the suspension: gypsum (5 °C/10 °C)								
	B1	B2	B3	B4	C1	C2	C3	C4
$Na_2O_{eq.}$ = 0 wt.%								
Gypsum	X/X	–/–	X/X	X/X	X/X	X/X	X/X	X/X
Calcite	X/X	X/X	X/X	X/X	X/X	X/X	X/X	X/X
Aragonite	–/–	–/–	–/–	–/–	X/X	–/–	–/–	–/–
Ettringite	–/–	X/X	X/X	X/X	–/–	X/X	X/X	X/X
Thaumasite	X/X	X/X	X/X	X/X	–/–	X/X	X/X	–/–
Woodfordite (solid solution)	–/–	X/X	–/–	–/–	–/–	–/–	–/–	–/–
pH values	12.7/12.7	12.2/12.9	13.0/12.7	12.8/12.6	12.2/11.7	11.8/12.0	11.6/11.8	11.4/11.7
$Na_2O_{eq.}$= 0.5 wt.%								
Gypsum	X/X	X/X	X/X	X/X	X/X	X/X	X/X	X/X
Calcite	X/X	X/X	X/X	X/X	X/X	X/X	X/X	X/X
Aragonite	–/–	–/–	–/–	–/–	X/X	–/–	–/–	–/–
Ettringite	X/X	X/X	X/X	X/X	–/–	X/X	X/X	X/X
Thaumasite	–/–	X/X	X/X	X/X	–/–	X/X	X/X	–/–
pH values	12.9/12.9	13.1/12.7	13.0/12.9	13.0/12.7	12.2/12.0	12.0/11.8	12.2/11.6	11.7/11.8
Source of sulphate in the suspension: Na_2SO_4 (5 °C/10 °C)								
$Na_2O_{eq.}$ = 0 wt.%								
Gypsum	–/–	–/–	–/–	–/–	–/–	–/–	–/–	X/X
Calcite	X/X	X/X	X/X	X/X	X/X	X/X	X/X	X/X
Aragonite	–/–	–/–	–/–	–/–	X/X	–/–	–/–	–/–
Ettringite	X/X	X/X	X/X	X/X	–/–	X/X	X/X	X/X
Thaumasite	X/–	X/X	–/–	X/X	–/–	–/–	–/–	–/–
pH values	13.3/12.9	13.0/13.1	13.3/13.0	13.3/12.9	12.4/12.3	12.5/12.3	12.9/12.4	12.5/12.2
$Na_2O_{eq.}$ = 0.5 wt.%								
Gypsum	–/–	–/–	–/–	–/–	–/–	–/–	–/–	X/X
Calcite	X/X	X/X	X/X	X/X	X/X	X/X	X/X	X/X
Aragonite	–/–	–/–	–/–	–/–	X/X	–/–	–/–	–/–
Ettringite	X/–	X/X	X/X	X/X	–/–	X/X	X/X	X/X
Thaumasite	X/–	X/X	–/–	X/X	–/–	–/–	–/–	–/–
pH values	13.3/13.0	13.0/13.0	13.2/13.0	13.1/13.0	12.5/12.3	12.6/12.4	12.6/12.4	12.5/12.2

Presence of phase is denoted by X.

of thaumasite were identified only after 356 days of storage in mixtures with small amounts of Al_2O_3 and poorly developed ettringite peaks. Furthermore, it was observed that more thaumasite formed when more aluminate was available. The mineral phases in the solid material of suspensions A after 365 days of storage are presented in Table 2. However, only traces of thaumasite were detected after 1 year in mixtures containing fly ash when gypsum was used as a source of sulphate. The ettringite diffraction peaks are weak like those of thaumasite. Thaumasite was not identified for suspensions with fly ash and Na_2SO_4 as sulphate source. Comparing the mixtures A2 (alite) and A6 (80% alite plus 20% fly ash), no difference at the amount of thaumasite was detected. Hence, the mixtures with fly ash were not more susceptible to the formation of thaumasite than pure alite. These observations agree with the studies of Nobst and Stark [8]. These authors also observed only a minor effect of fly ash on the formation of thaumasite in mixtures with 20 wt.% fly ash in hydrated SR cement after 200 days.

It is especially interesting that thaumasite started to form already after 14 days in all samples made with paste A3. This mixture contained the highest amount of Al_2O_3 (3.7 wt.%) compared to the others. The amount of gypsum added to the paste corresponded to complete reaction with the available aluminate to form ettringite during the hydration process. Therefore, it can be assumed that a certain amount of ettringite is essential for the rapid formation of thaumasite. In fact, Nobst and Stark [8] demonstrated experimentally that the amount of thaumasite is directly proportional to the total amount of Al_2O_3. They suggested that an ettringite-related structure operates as a precursor for the incorporation of silicon in thaumasite. However, they could not explain the exact mechanisms of this process.

Diffraction diagrams for three selected samples of different suspensions with $Na_2O_{eq.}$ = 0.5 wt.% after 365 days of storage are presented in Fig. 3. All the suspensions were prepared with gypsum and calcite and stored at 5 °C. The first mixture A1 did not contain aluminate, but the suspension included initially all components necessary for the formation of thaumasite. However, thaumasite was not detected by XRD even after 365 days. The second diagram for mixture A5 contains distinct peaks for thaumasite and ettringite in addition to C_4AF, gypsum and alite. The most intense peaks for thaumasite were detected in samples made with mixture

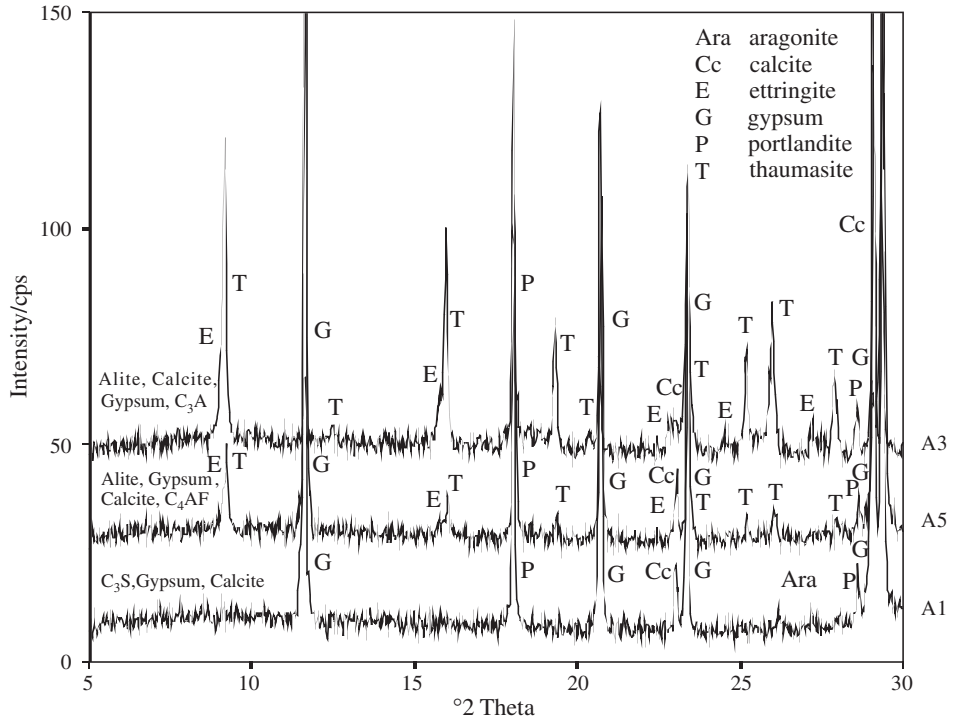

Fig. 3. Selected samples for suspensions with A1, A3 and A5 after 365 days. Storage at 5 °C, gypsum as source of sulphate.

A3. Rietveld analysis shows that there is half as much thaumasite in sample A5 as in sample A3. This indicates that the formation of thaumasite is coupled to the formation of ettringite. It appears that larger amounts of gypsum in the initial paste which led to larger amounts of ettringite in the hydrated mixture promoted the formation of thaumasite in the suspension.

3.2. Results for suspensions B and C with additional SiO_2

In general, the behaviour of samples based on mixtures B and C was similar to mixtures A. However, there was no thaumasite observed in suspensions with high amounts of nanosilica (C1–C4) and Na_2SO_4 as sulphate source. It is observed that more thaumasite forms at higher ettringite availability. The mineral phases in mixtures B and C are listed in Table 3.

However, an ettringite–thaumasite solid solution with X-ray peaks between those of these phases was detected in two suspensions B2, Fig. 4. The mixture B2 is characterised by a high degree of ettringite formation during the hydration process and by a larger content of C–S–H phases due to the amount of nanosilica. Furthermore, the paste was prepared without potassium addition; gypsum was added to the suspension, see Fig. 1. The exact cause for the woodfordite formation is, at present, uncertain.

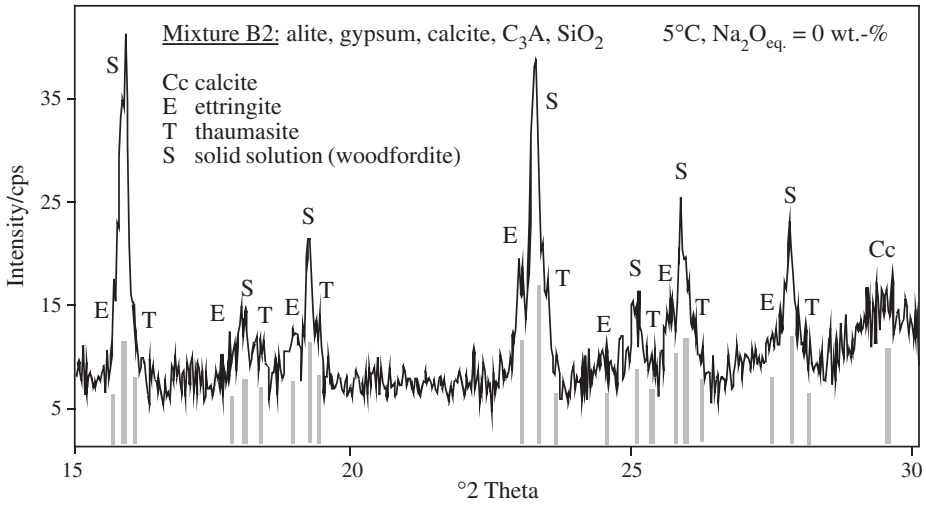

Fig. 4. Section of X-ray diffraction pattern of one sample of mixture B2 (alite, C_3A, SiO_2, gypsum, calcite) after 365 days.

Table 4
Lattice parameters a and c, d-spacings of ettringite from Moore and Taylor [21] in comparison with values for the solid solution (woodfordite) calculated by means of the Rietveld method

Ettringite (ICSD PDF number: 72-0646)					Solid solution (woodfordite)				
a=11.23 Å, c=21.50 Å					a=11.15 Å, c=21.11 Å				
d-spacing (Å)	Intensity (cps)	h	k	l	d-spacing (Å)	Intensity (cps)	h	k	l
5.7713	58	1	0	3	5.6874	56	1	0	3
5.6300	414	1	1	0	5.5748	626	−1	−1	0
5.3700	2	0	0	4	5.2783	0.6	0	0	4
4.9864	130	−1	−1	2	4.9297	153	−1	−1	2
					4.9297	12	−1	−1	−2
4.8757	24	2	0	0	4.8280	47	2	0	0
4.7547	19	2	0	1	4.7065	19	2	0	1
4.7039	225	1	0	4	4.6315	286	1	0	4
4.4396	7	2	0	2	4.3906	11	2	0	2
4.0300	41	2	0	3	3.9812	60	2	0	3
3.9314	12	1	0	5	3.8689	7	1	0	5
3.8858	308	−1	−1	4	3.8329	221	−1	−1	4
					3.8329	217	−1	−1	−4
3.6857	29	2	1	0	3.6496	45	−2	−1	0
3.6326	14	−2	−1	1	3.5963	1	−2	−1	−1
					3.5963	19	−2	−1	1
3.6097	67	2	0	4	3.5625	107	2	0	4
					3.5189	2	0	0	−6
3.4861	139	−2	−1	2	3.4493	134	−2	−1	−2
					3.4493	68	−2	−1	2
3.3606	2	1	0	6	3.3062	2	1	0	6
3.2770	35	−2	−1	3	3.2399	23	−2	−1	3
					3.2399	38	−2	−1	−3
3.2504	74	3	0	0	3.2186	148	3	0	0
					3.1785	0.3	2	0	5
3.2138	6	3	0	1	3.1819	8	3	0	1
3.1111	4	3	0	2	3.0787	7	3	0	2
					3.0019	2	−2	−1	4
					3.0019	2	−2	−1	−4
3.0209	26	−1	−1	6	2.9757	35	−1	−1	6

The Rietveld method, which is a full pattern-fitting method of X-ray powder diffraction data, was used to obtain lattice parameters a and c as well as d-spacings of the solid solution (woodfordite). The ettringite data of Moore and Taylor [21] provided the basis for the Rietveld refinement of the solid solution. The application of thaumasite data from Edge and Taylor [22] as basis did not yield plausible results. In Table 4, the solid solution values are compared with those published by Moore and Taylor [21] for ettringite. The solid solution is trigonal (space group P31c). The Rietveld fit is very good since the goodness-of-fit parameters R_{wp}=14.54 wt.% and R_{exp}=12.42 wt.% agree well. There were some minor problems fitting the broadness of the peaks and the peak overlap of the phases. It was, therefore, not possible to determine crystallite size and micro-strain.

The lattice parameters a and c (Table 4) are within the miscibility gap of the ettringite–thaumasite system as postulated by Barnett et al. [20]. Two other examples of solid solutions located in the miscibility gap have been reported by Torres et al. [23] and Barnett et al. [24]. The latter authors determined the chemical composition of a field sample subjected to a strong sulphate solution with a=11.165 Å and c=10.553 Å. They found more sulphate than expected for the stoichiometry of thaumasite. Thus, sulphate incorporation could also be the reason for the lattice parameters observed in the present study.

3.3. Comparison between suspensions A, B and C

Comparison of XRD results for similar mixtures with different amounts of SiO_2 to obtain different C/S ratios (A=3.0, B=1.7 and C=1.0 in Table 1) shows a delay of the formation of thaumasite at lower C/S ratios when Na_2SO_4 was used as a sulphate source. Thaumasite was detected only in traces in such mixtures C after 365 days. This trend was confirmed by the removal of sulphate from the storage Na_2SO_4 solution and the uptake of sulphate by the particles. The uptake of sulphate by the C–S–H phases and consequent formation of thaumasite for mixtures A3, B2 and C2 was calculated from the results of the chemical analysis of the storage solution, Fig. 5. At all times, the sulphate uptake increased from C2, B2 and A3 and from C2 via B2 to A3 even though the initial sulphate concentration of the solution is the same in all cases. Comparing the three suspensions, mixture C2 contains the highest amount of nanosilica and has therefore the highest potential for the formation of C–S–H phases. However, there was no sign of thaumasite in suspension even after 365 days. Therefore, the minor increase

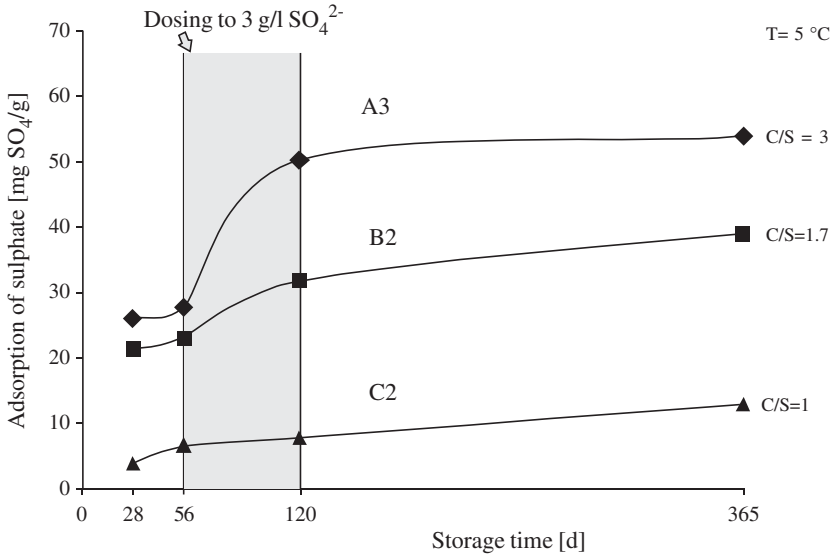

Fig. 5. Uptake of sulphate by solid phases from Na_2SO_4 in storage solution (suspensions A3, B2 and C2).

in sulphate content of mixture C2 could be explained by the assimilation of sulphate by the C–S–H phases. Mixture B2 possesses smaller amounts of nanosilica and yields thaumasite in suspension. Thus, the larger increase of sulphate content of the solid phases in comparison to C2 is due to the formation of thaumasite in addition to the absorption of sulphate by C–S–H phases. Mixture A3 contains alite instead of nanosilica and shows the highest amount of thaumasite in suspension. This is reflected by the high sulphate uptake from the solution. After 56 days, the concentration of sulphate in the solution was near equilibrium at roughly 200 mg/l for mixtures A3 because there is only a flat increase in sulphate uptake between 28 and 56 days.

After 56 days, sulphate was added to give a concentration in the suspensions of 3 g/l SO_4^{2-}. The subsequent sharp increase in sulphate uptake for mixtures A3 and B2 is connected with increased formation of thaumasite. Between 120 and 365 days, the curves level off as the equilibrium solution concentration is nearly reached.

The results of the Rietveld analyses for C–S–H and thaumasite in the solid phases are in Fig. 6. The amount of C–S–H as an amorphous content was determined by addition of an internal standard. The goodness-of-fit parameters ranged between $R_{wp}=11.20$ wt.% with $R_{exp}=9.14$ wt.% and $R_{wp}=14.57$ wt.% with $R_{exp}=9.87$ wt.%. Between 28 and 56 days, the amount of C–S–H increases while the thaumasite content stays nearly constant. On addition of sulphate (after 56 days), it is apparent that the amount of thaumasite increases while the amount of C–S–H decreases. This shows clearly that the SiO_2 for the formation of thaumasite is associated with the decomposition of C–S–H phases. Furthermore, in agreement with the behaviour in Fig. 3, the amounts of thaumasite and C–S–H stay nearly constant between 120 and 365 days. The C–S–H phases of suspension C2 show a trend similar to the other curves of C–S–H phases, but the content of thaumasite is apparently under the detection limit for XRD (estimated ca. 1 wt.%).

3.4. Investigations with ESEM and TEM

The solid solution phase woodfordite between thaumasite and ettringite was observed only in the case of mixture B2. It was identified together with ettringite and thaumasite in samples with $Na_20_{eq.}=0$ wt.% at storage temperatures of 5 and 10 °C and gypsum as sulphate source after 56,120 and 365 days. Rietveld analysis revealed that it is a phase similar to thaumasite. Such samples are particularly suitable for investigations of epitaxial growth between ettringite, woodfordite and

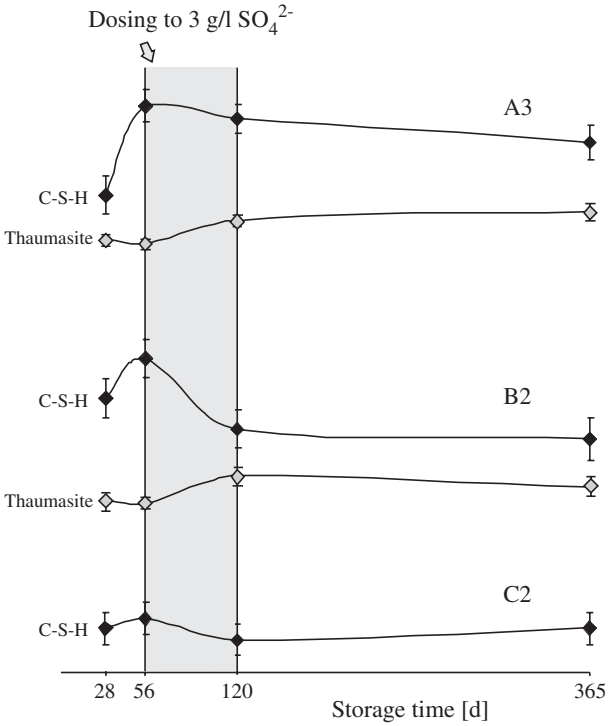

Fig. 6. Thaumasite and C–S–H phases development over 356 days calculated from XRD analysis with the Rietveld method.

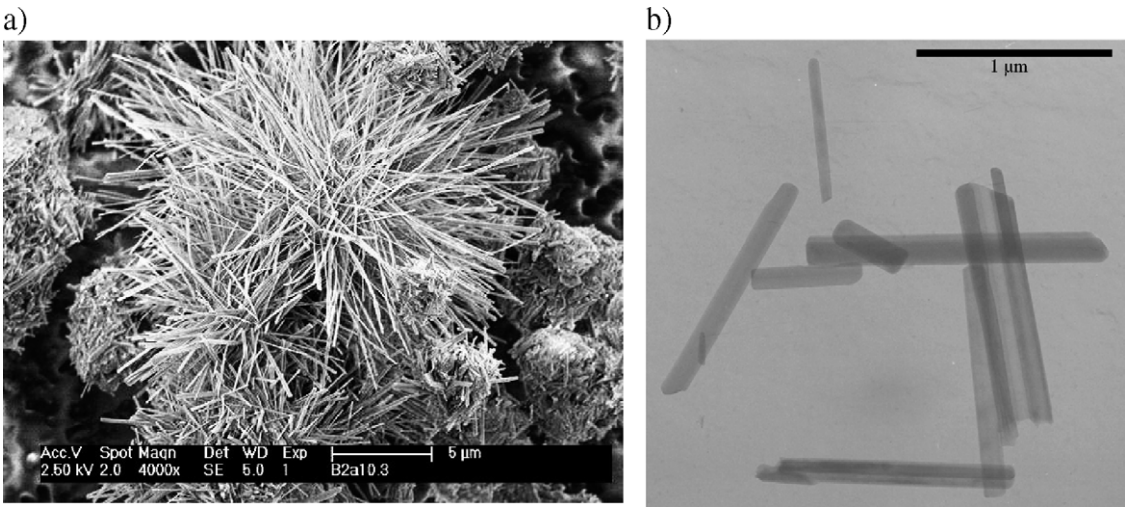

Fig. 7. (a) SEM image of spicular crystals of thaumasite/woodfordite of samples B2 (alite, C_3A, SiO_2, gypsum, calcite), (b) TEM image of spicular crystals of thaumasite/woodfordite of samples B2 (alite, C_3A, SiO_2, gypsum, calcite).

thaumasite. At first, an image with ESEM was taken (Fig. 7a). Due to its higher resolution TEM was used to study individual crystals (Fig. 7b). The images show thin translucent spicular crystals which form neither intergrowth nor twin crystals. Moreover, there are no visible signs of disintegration at the rims or at the surface of crystals.

Lattice planes parallel to the crystallographic *c* axis are usually studied to reveal lattice defects in single crystals. However, due to the instability of the material in the electron beam, this concept could not be applied. Investigations with EDX on individual crystals were carried out to analyse the distribution of Al^{3+} and Si^{4+}. These experiments were also difficult to perform because of the small thickness of the needles. In most cases the signal strength was insufficient for analysis. However, the analysis of a thicker crystal showed regions with and without Al^{3+} which could be evidence for intergrowth.

3.5. Investigation of the effect of ettringite on thaumasite formation

For further investigations on the mechanism of thaumasite formation, samples made with paste A3 were chosen for Rietveld analysis because of their ability to form thaumasite at an early age. In Fig. 8, the amount of thaumasite is plotted as function of the amount of ettringite.

The following observations are made.

1) Thaumasite is already detectable at more than 10 wt.% after 14 days. The amount of thaumasite increases continuously to a value of 63±2 wt.% in mixtures with gypsum as sulphate source whereas they seem to vary randomly within a range of 12–22±2 wt.% in mixtures of additional Na_2SO_4.

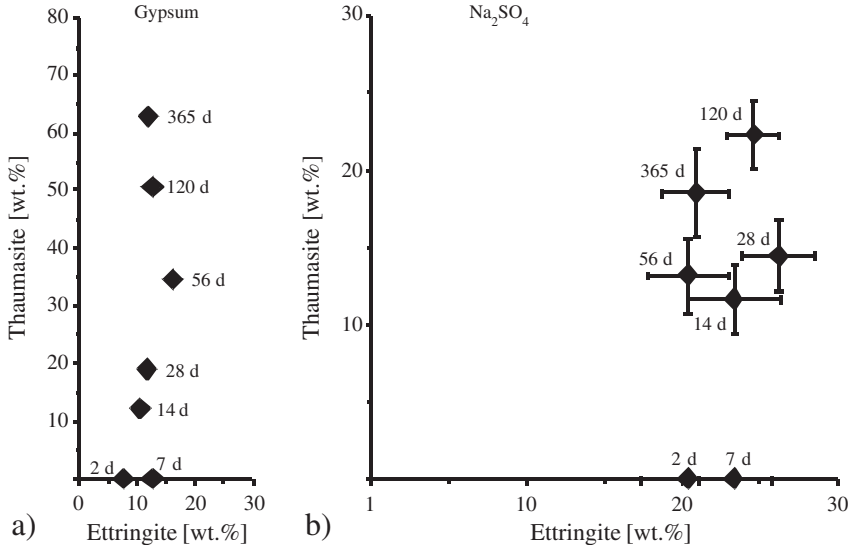

Fig. 8. Amount of thaumasite vs. ettringite after sampling between 2 and 365 days, in (a) standard deviations correspond to rectangle sizes and in (b) standard deviations are marked by bars.

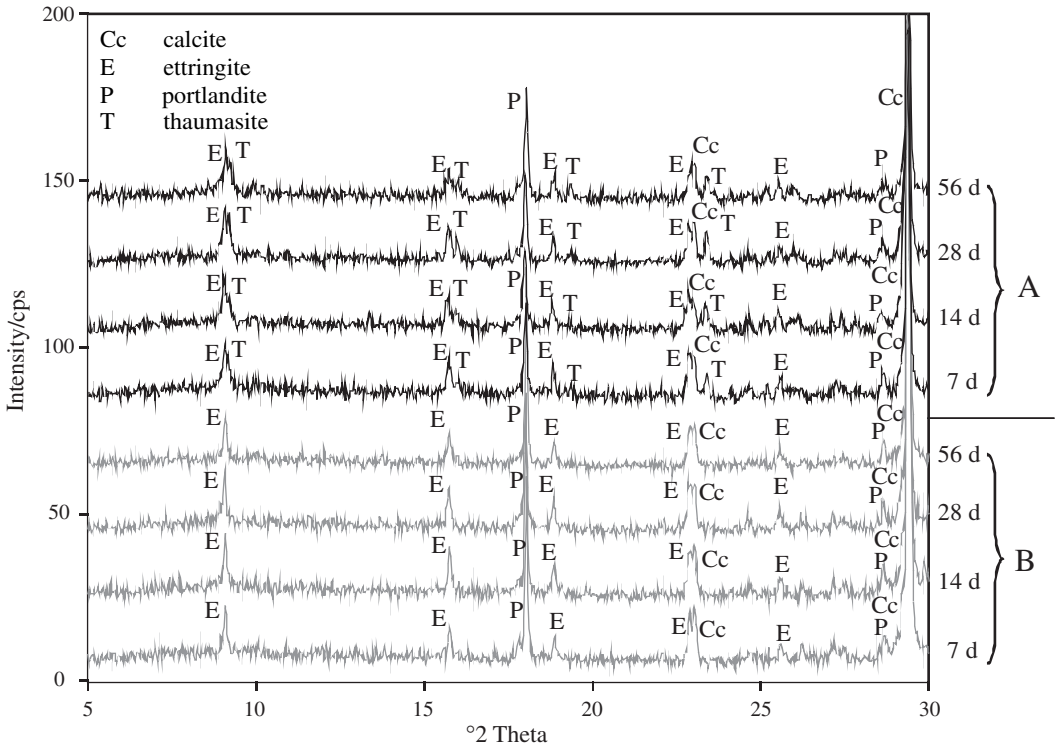

Fig. 9. Hydrated C_3S+calcite, with 30 wt.% ettringite and stored in suspension at 5 °C, (A) suspensions with added Na_2SO_4, (B) equivalent mixtures without additional sulphate.

2) For both types of sulphate source, the amount of ettringite remains constant within a range of about ±5 wt.%.
3) This behaviour occurred for all samples made with mixture A3 regardless of different $Na_2O_{eq.}$ or the temperature of storage.

In additional investigations, the suspension made with A1 (C_3S) which did not show any sign of thaumasite after 365 days was doped with synthetic ettringite. The preparation and storage procedures are described in Section 2.3. The results of these experiments can be summarised as follows:

1) Mixtures with 10 and 30 wt.% ettringite, but without additional sulphate (Na_2SO_4), did not show thaumasite formation within 56 days.
2) Thaumasite was detected in mixtures with ettringite and additional sulphate after only 7 days (Fig. 9).
3) Woodfordite was not detected in the mixtures.
4) No decrease in the amount of ettringite was observed by means of Rietveld analysis in mixtures containing thaumasite. The amounts of ettringite and thaumasite are listed in Table 5.

Table 5
Amounts of ettringite and thaumasite for mixtures C_3S, calcite and 30 wt.% ettringite calculated by means of Rietveld method

Storage time (days)	Ettringite (wt.%)	Thaumasite (wt.%)	R_{wp}	R_{exp}
7	26.0±2.4	12.3±1.9	18.31	14.37
14	25.3±2.5	17.3±1.9	17.39	14.51
28	24.9±2.3	18.8±1.8	17.10	14.19
56	24.5±2.7	19.7±2.0	18.24	15.62

4. Conclusions

The solid solution woodfordite whose composition lies between ettringite and thaumasite was detected after 56 days in only 2 out of 120 cases investigated. The lattice parameters of this phase (a=11.15 Å, c=21.11 Å) are situated within the miscibility gap postulated by Barnett et al. [20]. This could be explained by the incorporation of more sulphate ions. No transformation of ettringite into woodfordite or woodfordite into thaumasite was observed. This indicates clearly that thaumasite is not formed via the woodfordite route.

Since all the suspensions which were prepared with the stoichiometric composition of thaumasite, but without aluminate, did not contain thaumasite after 1 year, the formation of thaumasite without ettringite and direct from the solution is extremely slow or unlikely. It was found that ettringite considerably controls the rate of thaumasite formation. Moreover, the dissolution of C–S–H and, linked to it, the formation of thaumasite were observed.

Thus, two possible ways of thaumasite formation postulated by Crammond [3] remain. At first, thaumasite can be formed through a topochemical interchange of [Si] for [Al] and $[CO_3^{2-}+SO_4^{2-}]$ for $[SO_4^{2-}+H_2O]$. However, since topochemical interchange occurs at the outermost molecular layer of ettringite single crystals, this theory cannot explain the rapid formation of large amounts of thaumasite. The second theory of

thaumasite formation after Crammond [3] indicates that thaumasite uses ettringite as a template for its initial nucleation which, in view of the present results, we consider more likely.

We suggest that thaumasite formation occurs through the heterogeneous nucleation of thaumasite on the surface of ettringite, due to the structural similarities of these minerals, followed by epitaxial growth of thaumasite on lower layers from its solution components. The change from ettringite to thaumasite parallel the crystallographic *c*-axis may also explain the present TEM observations.

Acknowledgements

The authors thank Dr. Hanzlik and Dr. Chatziagorastou for taking microphotographs. Furthermore, we thank Dr. Beddoe and Dr. Hanzlik for helpful discussions. The authors express their thanks to the German Research Foundation (DFG) for financial support.

References

[1] S. Sahu, S. Badger, N. Thaulow, Mechanisms of thaumasite formation in concrete slabs on grade in Southern California, Cem. Concr. Compos. 25 (2003) 889–897.
[2] Thaumasite Expert Group, The thaumasite form of sulfate attack: risk, diagnosis, remedial works and guidance on new constructions, Report of the Thaumasite Expert Group, Dpt. of the Environment, Transport and the Regions, London, 1999.
[3] N.J. Crammond, The thaumasite form of sulphate attack in the UK, Cem. Concr. Compos. 25 (2003) 809–818.
[4] S.J. Barnett, C.D. Adam, A.R.W. Jackson, Solid solutions between ettringite, $Ca_6Al_2(SO_4)_3(OH)_{12}•26H_2O$, and thaumasite, $Ca_3SiSO_4CO_3(OH)_6•12H_2O$, J. Mater. Sci. 35 (2000) 4109–4114.
[5] D.E. Macphee, S.J. Barnett, Solution properties of solids in the ettringite–thaumasite solid solution series, Cem. Concr. Res. 34 (2004) 1591–1598.
[6] S.J. Barnett, D.E. Macphee, E.E. Lachowski, N.J. Crammond, XRD, EDX and IR analysis of solid solutions between thaumasite and ettringite, Cem. Concr. Res. 32 (2002) 719–730.
[7] S.J. Barnett, D.E. Macphee, N.J. Crammond, Extend of immiscibility in the ettringite–thaumasite system, Cem. Concr. Compos. 25 (2003) 851–855.
[8] P. Nobst, J. Stark, Investigations on the influence of cement type on the thaumasite formation, Cem. Concr. Compos. 25 (2003) 899–906.
[9] J. Bensted, Thaumasite-direct, woodfordite and other possible formation routes, Cem. Concr. Compos. 25 (2003) 873–877.
[10] J. Bensted, Mechanism of thaumasite sulphate attack in cements, mortars and concretes, ZKG Int. 12 (2000) 704–709.
[11] J. Bensted, Thaumasite—background and nature in deterioration of cements, mortars and concretes, Cem. Concr. Compos. 21 (1999) 117–121.
[12] S.A. Hartshorn, J.H. Sharp, R.N. Swamy, Thaumasite formation in Portland–limestone cement pastes, Cem. Concr. Res. 29 (1999) 1331–1340.
[13] M.E. Gaze, The effects of varying gypsum content on thaumasite formation in a cement:lime:sand mortar at 5 °C, Cem. Concr. Res. 27 (1997) 259–265.
[14] M.E. Gaze, N.J. Crammond, The formation of thaumasite in a cement: lime sand mortar exposed to cold magnesium and potassium sulfate solutions, Cem. Concr. Compos. 22 (2000) 209–222.
[15] S. Sahu, S. Badger, N. Thaulow, Mechanism of thaumasite formation in concrete, First International Conference on Thaumasite in Cementitious Materials, Paper No 68 (2002).
[16] I. Pajares, S. Martinez-Ramirez, M.T. Blanco-Varela, Evolution of ettringite in presence of carbonate, and silicate ions, Cem. Concr. Compos. 25 (2003) 861–865.
[17] E. Freyburg, A.M. Berninger, Field experiences in concrete deterioration by thaumasite formation: possibilities and problems in thaumasite analysis, Cem. Concr. Compos. 25 (2003) 1105–1110.
[18] M. Atkins, F.P. Glasser, A. Kindness, Cement hydrate phases: solubility at 25 °C, Cem. Concr. Res. 22 (1992) 241–246.
[19] F. Bellmann, J. Stark, Ein Beitrag zum Chemismus der Thaumasitbildung, 15, Intern. Baustofftagung Ibausil. 2 (2003) 0659–0671.
[20] S.J. Barnett, D.E. Macphee, N.J. Crammond, Extent of immiscibility in the ettringite–thaumasite system, Cem. Concr. Compos. 25 (2003) 851–855.
[21] A.E. Moore, H.F.W. Taylor, Crystal structure of ettringite, Acta Crystallogr., Sect. B 26 (1970) 386–393.
[22] R.A. Edge, H.F.W. Taylor, Crystal Structure of Thaumasite, $[Ca_3Si(OH)_6•12H_2O](SO_4)(CO_3)$, Acta Crystallogr., Sect. B 27 (1971) 594–601.
[23] S.M. Torres, C.A. Kirk, C.J. Lynsdale, R.N. Swamy, J.H. Sharp, Thamasite–ettringite solid solutions in degraded mortars, Cem. Concr. Res. 34 (2004) 1297–1305.
[24] S.J. Barnett, D.E. Macphee, N.J. Crammond, Solid solutions between thaumasite and ettringite and their role in sulphate attack, Concr. Sci. Eng. 3 (2001) 209–215.